NASA TECHNICAL NOTE

NASA TN D-4317
C. 1

NASA TN D-4317

A STUDY OF THE EFFECT
OF MEASUREMENT ERRORS
UPON A RANGE CONTROLLER
FOR AN ENTRY VEHICLE

by Jack A. White

Langley Research Center

Langley Station, Hampton, Va.

NATIONAL AERONAUTICS AND SPACE ADMINISTRATION • WASHINGTON, D. C. • JANUARY 1968

A STUDY OF THE EFFECT OF MEASUREMENT ERRORS UPON

A RANGE CONTROLLER FOR AN ENTRY VEHICLE

By Jack A. White

Langley Research Center
Langley Station, Hampton, Va.

NATIONAL AERONAUTICS AND SPACE ADMINISTRATION

A STUDY OF THE EFFECT OF MEASUREMENT ERRORS UPON
A RANGE CONTROLLER FOR AN ENTRY VEHICLE

By Jack A. White
Langley Research Center

SUMMARY

A study of a range controller for an entry vehicle has been made. Three basic path trajectories to simulate short-range entries, medium-range entries (in which the vehicle pulls up to less dense atmosphere after the initial dive into the atmosphere), and long-range entries requiring a skip maneuver were selected for the study. The range controller used a bang-bang control during the initial dive into the atmosphere and during the pull-up phase for medium- or long-range entry. Control during the other phases of the trajectory was achieved by a linear-type controller that is dependent upon the solution of desired altitude as a function of desired range.

A random number procedure was used to determine the effect of random errors in measuring the vehicle velocity, altitude, and rate of change of altitude upon the effectiveness of the range controller to control the vehicle to the desired range.

Results of this study show that the range controller was able to control the vehicle from the entry point for angular ranges varying from 18° to 250°. Results of the error analysis show that the range controller was much more sensitive to measurement error when a medium- or long-range entry was desired than when a short-range entry was desired. The controller had about the same sensitivity to measurement errors for medium-range and long-range entries.

INTRODUCTION

In recent years numerous procedures for the control of an entry vehicle into the earth's atmosphere have been presented. One comprehensive review of these entry control methods, recently compiled in reference 1, has discussed the procedures and techniques from a control logic standpoint. The guidance problem can be reduced to two simple questions:

(1) What trajectory should be flown in order to arrive safely at the desired destination?

(2) What control logic should be used to attain this trajectory?

The first question implies that the trajectory selected must be one that does not overheat or overstress the vehicle and its occupants. Once this trajectory is selected, the second question becomes one of formulating a control law to obtain it. In any workable control system, the control laws are formulated in such a manner that overshoot is held to a minimum since the price paid for a large overshoot is either an uncontrolled skip or overdeceleration.

For the work reported in reference 2, only two state variables were required to define a switching curve to determine when a positive or a negative control force should be used in order to control an entry vehicle to a desired altitude and flight-path angle. The results of the study show that the equation used as the switching curve for the bang-bang controller gave an excellent prediction as to when a control maneuver should be made. For short-range entries, the bang-bang controller effectively eliminated overshoot so that neither uncontrolled skips or overdeceleration was incurred for a wide range of entry conditions. The study reported in reference 2 was limited to direct descent entries and to longitudinal range control.

The purpose of the present study is to modify the control logic to include entries requiring skip maneuvers. The control logic modification also includes lateral range control. A random-number procedure is used to determine the effect of errors in velocity, altitude, and rate of change of altitude upon the ability of the controller to achieve a desired destination. The results of this study, shown as probability curves, are so presented that the probability of the space vehicle's missing the desired range by a given amount can be read directly from the curves.

SYMBOLS

a_D deceleration of vehicle, g units

B constant used in exponential approximation of atmospheric density, meters

C constant used in switching logic, kilometers

C_D drag coefficient

C_L lift coefficient

C_L* arbitrary value of C_L selected for the vertical component of lift for the constant C_L control phase

g acceleration due to gravity, kilometers/second^2

G_1 gain factor used with Δh in controller, radians/kilometer

G_2 gain factor used with $\dot{h}$ in controller, radians-sec/km

h altitude of vehicle, kilometers

h_d desired altitude for constant-altitude phase of desired mode of flight, kilometers

Δh increment in altitude $\left(h_d - h\right)$, kilometers

k constant used with switching curve

m mass of vehicle, kilograms

r radius of earth, kilometers

S lifting-surface area, meters^2

t time, seconds

V velocity of vehicle, kilometers/second

V_2 velocity of vehicle at beginning of constant C_L phase, kilometers/second

V_3 velocity of vehicle at beginning of pull-up phase for the second desired mode of flight, kilometers/second

V_4 velocity of vehicle at beginning of pull-up phase for the third desired mode of flight, kilometers/second

x longitudinal range, nautical miles

y lateral range, nautical miles

y_d lateral range to be covered during entry, nautical miles

γ flight-path angle, degrees or radians

γ_d desired flight-path angle for a given altitude, degrees or radians

γ_R magnitude of γ that can be arrested by using $|C_L|$ between present altitude and desired altitude, radians

η angular travel from entry point of vehicle above earth, degrees or radians

η_d desired angular travel of vehicle, degrees or radians

ρ_c constant used for exponential approximation of density of atmosphere, kilograms/meter^3

ϕ roll angle, degrees

ϕ_c angle of roll command, degrees

ψ heading angle, degrees or radians

σ_V standard deviation of error in V, meters/second

σ_h standard deviation of error in h, meters

$\sigma_{\dot{h}}$ standard deviation of error in $\dot{h}$, meters/second

Subscripts:

o   initial conditions at beginning of dive phase

S   skip conditions at upper limit of usable atmosphere

A dot above a quantity denotes rate of change of variable with respect to time.

METHOD OF ANALYSIS

Control Modes and Trajectory Phases

Three desired modes of flight as shown in sketches A, B, and C were assumed in order to include entries that required skip maneuvers. The basic mode of flight, the same as that assumed in reference 2, is an initial dive into the atmosphere, which is followed by a constant-altitude trajectory until equilibrium flight conditions for an assumed lift coefficient are achieved and a subsequent constant-lift-coefficient trajectory to the desired point on the earth's surface. (See sketch A.) This mode of flight allows an analytical

expression for desired altitude as a function of desired range. Thus, the basic mode of flight is the desired mode of flight for short-range entries where the desired altitude for the constant-altitude phase of the trajectory is always below the maximum altitude where aerodynamic forces are available to prevent the vehicle from skipping out of the atmosphere.

The second assumed mode of flight (sketch B) is an initial dive into the atmosphere, which is followed by a short constant-altitude trajectory and then a pull-up to a higher altitude, where a constant-altitude trajectory is maintained until equilibrium flight conditions for an assumed lift coefficient are achieved, and finally a constant lift-coefficient trajectory to the desired destination. This mode of flight is the desired mode of flight for direct-descent entries where the desired altitude for the basic mode of flight is above the altitude where aerodynamic forces are available to prevent a skip and the vehicle therefore must fly at a lower altitude until excess velocity is bled off in order to insure controllability in less-dense atmosphere.

The third assumed mode of flight (sketch C) is an initial dive into the atmosphere, which is followed by a constant-altitude trajectory and then a pull-up and exit from the atmosphere where the vehicle will coast until it reenters the atmosphere, after which the vehicle follows the basic mode of flight to the desired point on the earth's surface. This mode of flight is the desired mode of flight when a skip maneuver is required in order to achieve the desired longitudinal range.
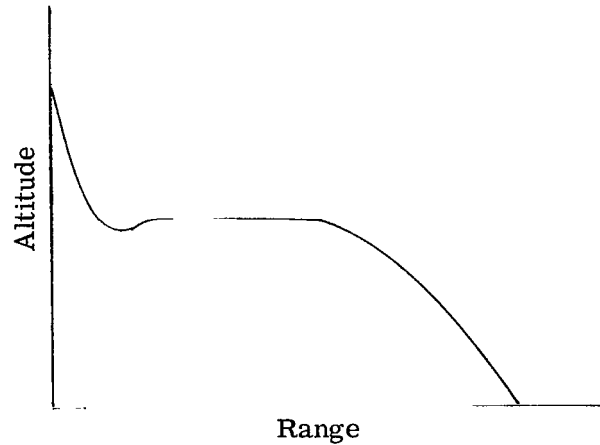
Sketch A.- Flight mode I.
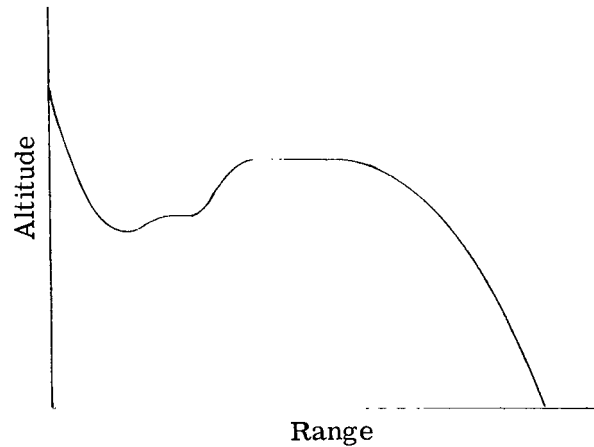
Sketch B.- Flight mode II.
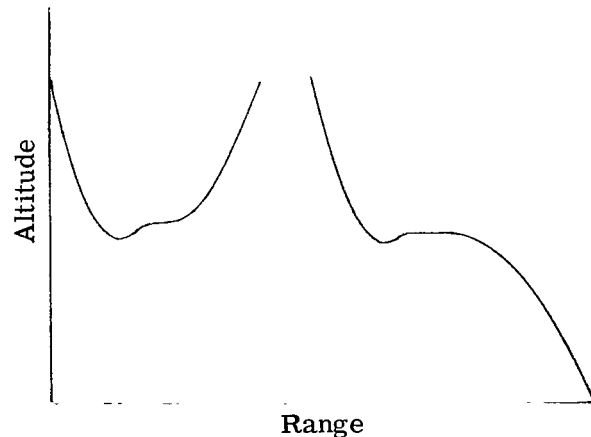
Sketch C.- Flight mode III.

5

Each of the three desired trajectories is divided into several control phases. The first trajectory is divided into the following three phases: the dive phase, which begins at the initial point of entry and ends when desired level-flight conditions are achieved; the constant-altitude phase, which covers the portion of the entry trajectory where constant altitude is maintained; and the constant C_L phase which covers the remainder of the entry trajectory. The second desired trajectory is divided into the following five phases: the dive phase; a short constant-altitude phase where the excessive velocity is bled off; the pull-up phase where the vehicle pulls up and levels off at a higher altitude; the second constant-altitude phase; and the constant C_L phase. The third desired trajectory has the following phases: the dive phase; the constant-altitude phase having a duration that is dependent upon desired atmospheric exit conditions; the pull-up phase, which ends when the vehicle exits from the atmosphere; the coast phase, which covers the portion of the trajectory outside the usable atmosphere; the second dive phase; the second constant-altitude phase; and the constant C_L phase.

The dive phase of the three desired entry trajectories is controlled by selecting such direction of maximum lift that at the end of the dive phase, level-flight conditions are achieved at the desired altitude.

Each of the constant-altitude phases of the three desired trajectories is controlled by a linear controller for which the appropriate amount of lift to maintain level flight can be modified by altitude error and rate of change of altitude.

The pull-up phase of the second and third desired trajectories is controlled by using maximum positive lift until the time when the direction of lift changes to negative in order to reduce the flight-path angle to the desired value at the desired altitude.

No control is used during the coast phase of the third desired trajectory. The vehicle is assumed to have exited from the atmosphere on an elliptical orbit. Standard elliptical orbital equations were used to calculate the range covered and the time required for the portion of the trajectory outside the atmosphere.

The constant C_L phase of the desired trajectories begins when equilibrium flight conditions for an assumed lift coefficient are achieved. In general, the vehicle will not fulfill all the requirements for equilibrium flight at the beginning of the constant C_L phase, and therefore the vehicle will not be on the desired trajectory. Hence, at two intermediate altitudes the lift coefficient may be changed by increments of 0.1 by a suitable roll command if the vehicle is not on the desired trajectory.

In the present study, the vehicle is assumed to be trimmed at a constant angle of attack, and lift control is obtained by rolling so that the drag coefficient is constant. Lateral-range control is achieved by a simple logic based upon rolling the vehicle in the proper direction during the constant-altitude and the constant C_L phases of the reentry trajectory.

Equations

The motion of a space vehicle entering the earth's atmosphere from outer space may be described by the following equations, under the simplifying assumptions of a spherical nonrotating earth and constant gravity:

$$\dot{h} = V \sin \gamma \tag{1}$$

$$\dot{\gamma} = K_1 V e^{-h/B} C_L \cos \phi - \frac{g}{V} \cos \gamma \left(1 - \frac{V^2}{gr}\right) \tag{2}$$

$$\dot{V} = -K_1 V^2 e^{-h/B} C_D - g \sin \gamma \tag{3}$$

where

$$K_1 = \frac{\rho_c S}{2m}$$

The angular range along the surface of the earth may be expressed by

$$\dot{\eta} = \frac{V}{r} \cos \gamma \tag{4}$$

This angular range can be broken down into longitudinal and lateral range by the following relations:

$$\dot{\psi} = K_1 V e^{-h/B} C_L \sin \phi \tag{5}$$

$$\dot{x} = V \cos \gamma \cos \psi \tag{6}$$

$$\dot{y} = V \cos \gamma \sin \psi \tag{7}$$

Switching-curve equation.- In order for the space vehicle to reach the desired values of γ and h simultaneously at the end of the dive phase or pull-up phase of the desired trajectory, it is necessary for the vehicle to roll from positive to negative lift or vice versa at some point along the trajectory. A switching curve that lies in the plane of the altitude flight-path angle was developed and reported in reference 2 for determining the switching point. The switching point for the present study was determined from the following expression (eq. (29) of ref. 2):

$$\gamma_R = \zeta \left[\gamma_d{}^2 - \zeta \frac{\rho_c S}{m} BC_L e^{-h_d/B} \left(1 - e^{\Delta h/B}\right) - \frac{2\Delta h}{r}\left(1 - \frac{gr}{V^2}\right) \right]^{1/2} \tag{8}$$

where Δh is the difference between the desired altitude and the instantaneous altitude and $\zeta = \Delta h/|\Delta h|$.

Desired constant-altitude equation.- An equation for the total range covered by the basic mode of flight was derived in reference 2. In the development of the range equation, the range covered during the dive phase was assumed equal to the range that would be covered if constant altitude were maintained during this phase. Also an empirical correction term was obtained to supplement the range covered during the constant C_L phase of the desired mode of flight. The range equation for the basic mode of flight is (eq. (20) of ref. 2):

$$\eta_d = \frac{m}{\rho_c SrC_D} \frac{1}{e^{-h_d/B}} \log\left[\frac{V^2}{gr}\left(1 + \frac{\rho_c C_L{}^* Sr}{2m} e^{-h_d/B}\right)\right]$$

$$+ \frac{1}{2}\frac{C_L{}^*}{C_D} \log\left(\frac{2m}{\rho_c rSC_L{}^*} e^{h_d/B} + 1\right) + e^{0.491\, h_d/B - 7.525} \tag{9}$$

where the third term represents the empirical correction for an earth entry when $C_L{}^* = 0.2$.

The constant altitude of the desired mode of flight for a given range was determined from equation (9) by using an iterative procedure.

Linear controller.- The linear controller which is used during the constant-altitude phase of the desired trajectory is represented by

$$\phi_c = \cos^{-1} \frac{2m\left(gr - V^2\right)}{\rho_c C_L rSV^2 e^{-h/B}} - 57.3\left(G_1 \Delta h + G_2 \dot{h}\right) \tag{10}$$

Control Logic

The control logic used with the bang-bang controller is dependent upon the value of the switching function γ_R. The control logic is stated: If $k\gamma_R - \gamma > 0$, then $\phi_c = 0^O$, but if $k\gamma_R - \gamma \leqq 0$, then $\phi_c = 180^O$ where k alternates from 1 to a value $0 \leqq k < 1$ each time the vehicle rolls. Alternating values of k are used in the control logic in order to prevent the vehicle from rolling excessively for a changing h_d and for measurement errors in V, γ, and h.

Lateral control is achieved by directing the lateral component of lift in the proper direction. In the present study it is assumed that the side force resulting from roll angles between 0° and 180° causes the heading angle ψ to increase in a positive direction and that resulting from roll angles between 180° and 360° causes ψ to decrease. The control logic was as follows: Initially the proper direction was selected (i.e., if it should be between 0° and 180° or between 180° and 360°) and this direction was maintained until $y = 0.7y_d$ and $\psi \geqq |15^O|$. At this point the direction of the side force was reversed and remained in this direction until ψ returned to zero. The condition $\psi \geqq |15|$ was included in the logic in order to prevent excessive rolling from small lateral ranges. After ψ has returned to zero, if $|y| < |y_d|$, the direction of side force is reversed and continues to switch each time ψ changes 10° until $|y| \geqq |y_d|$. The first time $|y| \geqq |y_d|$, the logic for the remainder of the trajectory was simply to reverse the direction of side force each time $\psi = |7.5^O|$. For the third desired mode of flight, the heading angle ψ was restrained between $\pm2.5^O$ at the time the vehicle exited from the atmosphere.

Each of the three desired modes of flight have several control phases. The dive phase is common to all three modes and ends when $\gamma = 0$ and $|h_d - h| \leqq C$. At this point the controller uses the following logic to select the correct mode of flight: Select mode I if $\eta < 40^O$, select mode II if $40^O \leqq \eta_d < 65^O$, and select mode III if $\eta_d \geqq 65^O$. Thus, for short ranges the system automatically shifts from the dive phase to the constant-altitude phase of desired mode I when $\gamma = 0$ and the error in altitude is equal to or less than an assumed value of C. The system continues in this control phase until the velocity is equal to or less than V_2 which is obtained by solving equation (2) (where $\dot{\gamma} = 0$) in terms of $C_L{}^*$.

At altitudes of 61.0 and 46.0 kilometers, which were arbitrarily selected along the constant C_L phase of the trajectory, the system uses a simple tabular selection to determine whether the vehicle is falling short or overshooting its target. Hence, the lift coefficient can be changed by an increment of 0.1 at these altitudes to correct the longitudinal range.

For a medium-range entry (mode II), the system continues in the constant-altitude phase until $V \leqq V_3$ (which was empirically selected at 9.3 kilometers/second) and then shifts to the pull-up phase. The altitude at which the vehicle attempts to achieve level-flight conditions during this phase is a constant obtained from $73.15 + 0.3048(\eta_d - 40)$. The system automatically shifts from the pull-up phase to the constant-altitude phase of mode I when $\gamma = 0$ and $|\Delta h| \leqq C$. After fulfilling this condition, the system shifts to a glide at constant C_L.

In order to control the range that the vehicle travels outside the atmosphere, the system attempts to control to specified skip conditions. These conditions are obtained by

assuming $\gamma_S = 2^O$ and calculating V_S for a desired range outside the atmosphere from the orbital equations. Thus, for long-range entries, the system will stay in the constant-altitude phase until $V \leqq V_4$ where $V_4 = V_S + 0.91$ and will then shift to the pull-up phase. In the pull-up phase, the system is trying to control to a γ of 2^O at the upper limit of the atmosphere. The pull-up phase ends when $h \geqq h_d$ and from the conditions at this point the portion of the trajectory outside the atmosphere is computed from the standard orbital equation. The vehicle then reenters the atmosphere and follows a dive phase, a constant-altitude phase, and a constant C_L phase similar to the desired flight mode I.

The following diagram (sketch D) shows the control phases for the three desired modes of flight. This diagram also indicates for each control phase: (1) which controller is used, and (2) the conditions that terminate the control phase.

Sketch D.

10
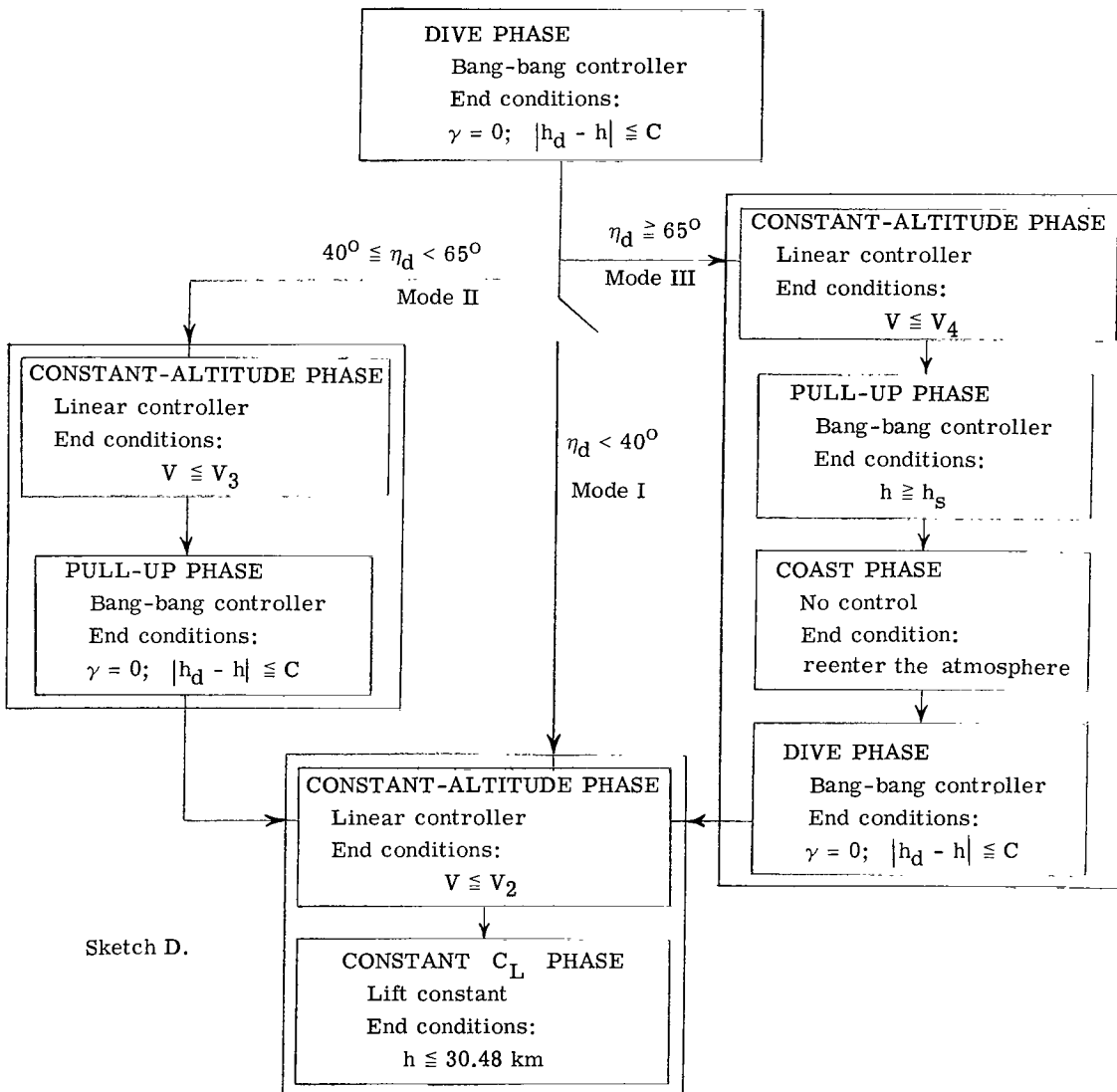
Measurement Errors

The control system requires a knowledge of the instantaneous value of velocity, altitude, and flight-path angle in order to command the proper value of the roll angle and in order to switch from one control phase to another. Thus, the entry vehicle must be capable of supplying the continuous values of these parameters to the control system.

In the present study the vehicle is assumed to be provided with instruments to measure velocity, altitude, and rate of change of altitude. From the measured values of V and $\dot{h}$, the flight-path angle is approximated by

$$\gamma = \frac{\dot{h}}{V}$$

and is used by the control system as the present value. The errors in measuring velocity, altitude, and rate of change of altitude are assumed to have a normal distribution. A digital computer subprogram for generating a random number was used to select errors to represent instrumentation inaccuracies in measuring the desired variables. Thus, the measured values of h, V, and $\dot{h}$ used by the control system are the true values of the variables plus random errors.

Digital Computer Study

The dynamics of the space vehicle and control system as described were simulated on a digital computer. The values of k used with the switching curve for the bang-bang controller were 1 and 0.7. The value of C used in the control logic to switch from the bang-bang controller to the linear controller was 2.0 kilometers. The gains used in the linear controller were $G_1 = 0.328$ radian/kilometer and $G_2 = -3.28$ radians/kilometer-second. The value for $C_L{}^*$ used in the range equation was 0.2.

A 2930-kilogram high-drag low-lift entry vehicle having a lifting area of 10 square meters was assumed for all entries simulated in the present study. It was assumed that the vehicle was trimmed at $C_L/C_D = 0.5$. Lift control was obtained by rolling the vehicle such that all the lift is: in an upward direction for $\phi = 0^O$, in a positive lateral direction for $\phi = 90^O$, in a downward direction for $\phi = 180^O$, and in a negative lateral direction for $\phi = 270^O$ (-90°). Instantaneous roll maneuvers were assumed.

The initial altitude for all entries was 91.44 kilometers (300,000 ft). This altitude was also assumed to be the upper limit of the usable atmosphere. The entries were terminated at $h = 30.48$ kilometers (100,000 ft) below which the high-drag low-lift vehicle has little or no maneuver capability.

RESULTS AND DISCUSSION

Time Histories for Assumed Flight Modes

Simulations of complete entries where no instrumentation inaccuracies were assumed for angular ranges from 18° to 250° were investigated. In the present study, the entry velocity was varied from 11 kilometers/second to 13.7 kilometers/second (approximately 36,000 ft/sec to 45,000 ft/sec) and the entry angle was varied from -3° to -6°. This range of entry angles represents initial flight-path angles that are steep enough for atmospheric capture, but shallow enough not to exceed a deceleration limit of 8g. The vehicle was controlled equally well for any combination of initial velocity and acceptable initial flight-path angle.

Lateral range was varied from -240 nautical miles to 240 nautical miles. In the present study, the lateral-range control was considered acceptable when the lateral range covered during the entry (where no instrumentation inaccuracies were assumed) was within ±10 nautical miles of the desired range. Thus, no attempt was made to obtain a tight control of the lateral range.

Figure 1 represents the switching curve computed (from eq. (8)) during the dive phase of a typical entry. This figure shows that positive lift should be used when γ is to the left of the switching curve and negative lift when γ is to the right of the switching curve.

Typical entries for an entry velocity of 12.2 kilometers/second (about 40,000 ft/sec) and entry angle of -5.5^O for the three desired modes of flight are presented in figures 2 to 4 as time histories. The desired lateral range for these three entries was 160 nautical miles and the desired angular ranges were 30°, 55°, and 150°, respectively. Three roll maneuvers were required for lateral control of the two trajectories that did not skip out of the atmosphere (figs. 2 and 3) and four roll maneuvers were required for the trajectory requiring a skip maneuver (fig. 4). The first lateral-control roll maneuver shown in figure 4 was required in order to limit the magnitude of the heading angle of the vehicle at the time of skip from the atmosphere.

Effect of Measurement Errors

Results of the simulation where random measurement errors were assumed are presented in figures 5 to 7 as range-error probability curves. These results based on 100 entries are so presented that the probability of the space vehicle missing the desired range by a given amount can be read directly from the figure. For example, when an angular range of 30° is desired and the sigma measurement-error values are $\sigma_V = 48$ meters/second, $\sigma_h = 0$, and $\sigma_{\dot{h}} = 0$, figure 5(a) shows that there is a 30 percent probability that the space vehicle will fall 5 nautical miles short of the desired

longitudinal range, and an 89 percent probability that the space vehicle will have obtained terminal conditions before overshooting the desired longitudinal range by 5 nautical miles.

Short-range entries.- Figure 5 shows the probability curves of range error for a desired angular range of $30°$ and a desired lateral range of 160 nautical miles. Figure 5(a) shows the effect of varying σ_V while σ_h and $\sigma_{\dot{h}}$ were set equal to zero. This figure indicates that a σ_V of about 40 meters/second would give a 100 percent probability of the range error being within 20 nautical miles. Figure 5(b) presents the results of varying σ_h while holding σ_V and $\sigma_{\dot{h}}$ at zero. The most noticeable effect shown is that when σ_h is increased, the probability of not reaching the desired range is increased. This effect is more pronounced in the lateral range error than in the longitudinal range error. The effect of varying $\sigma_{\dot{h}}$ while σ_V and σ_h are zero is shown in figure 5(c). These results indicate that an error in $\sigma_{\dot{h}}$ increases the probability of the space vehicle falling short of the desired range.

The solid line in figure 5(d) shows the results when errors were assumed to be present in all three variables. The sigma values used were: $\sigma_V = 40$ meters/second, $\sigma_h = 450$ meters, and $\sigma_{\dot{h}} = 32$ meters/second. The individual effect of each sigma error is repeated here for convenience. As expected, the combined effect of the measurement errors resulted in a wider spread of range errors.

Medium-range entries.- Figure 6 shows the probability curves of range error for a desired angular range of $55°$ and a lateral range of 160 nautical miles. Again, as for the short-range entries, the individual measurement errors were varied and then the combined effect is presented. From figure 3 it can be seen that a lateral-range error of about -7 nautical miles existed at the terminal point of the trajectory. This is the lateral-range error when no instrumentation errors are assumed. Hence, a lateral-range error of -7 nautical miles would be the nominal about which to evaluate the effect of instrumentation errors on the lateral-range control for results presented in figure 6.

The longitudinal-range probability curves for the cases where an error was assumed in velocity and no errors in altitude and rate of change of altitude, shown in figure 6(a), all obtained 100 percent at an error between 16 and 16.5 nautical miles. These same curves fail to show a trend of flattening out as 100 percent probability is approached as normally expected. In order to determine whether these two effects were a result of taking a small sampling rate, these three cases were rerun with 1000 samples to obtain the probability curves. The results of the 1000 samples showed a maximum positive range error of 16.5 nautical miles and the same low probability of falling short of the desired longitudinal range. The trends shown in figure 6(a) were thus concluded to be the result of errors in velocity and not of taking a small sampling rate.

The results shown in figure 6 indicate that if the range errors are to be kept within 30 nautical miles for medium-range entries, the sigma values of the instrumentation error will be σ_V = 4 meters/second, σ_h = 24 meters, and $\sigma_{\dot{h}}$ = 2 meters/second.

Long-range entries.- Figure 7 shows the range-error probability curves for a desired angular range of 150° and a desired lateral range of 160 nautical miles. Results of varying each of the three assumed instrumentation errors while holding the others at zero are presented and then the combined effect of the errors is presented.

The lateral range controller failed to obtain the full desired lateral range a large percentage of the runs for all errors investigated. Figure 7 shows that the longitudinal-range errors are about equally distributed about the desired range for all assumed errors.

For long-range entries, sigma values of the instrumentation errors of σ_V = 4 meters/second, σ_h = 32 meters, and $\sigma_{\dot{h}}$ = 2 meters/second are required in order to insure that the range errors are within 30 nautical miles a large percentage of the time.

Generalization.- The results presented in figures 5 to 7 are typical of the many probability curves obtained for various entry conditions, assumed measurement errors, and desired angular ranges. The results presented were selected on the assumption that a 30-nautical-mile error in longitudinal range would be unacceptable.

The error analysis shows that for range errors to be kept within 30 nautical miles, the sigma values of the measurement error were: For short-range entries, 40 meters/second in velocity, 450 meters in altitude, and 32 meters/second in rate of change of altitude; for medium-range entries, 4 meters/second in velocity, 24 meters in altitude, and 2 meters/second in rate of change of altitude; and for long-range entries, 4 meters/second in velocity, 32 meters in altitude, and 2 meters/second in rate of change of altitude.

CONCLUDING REMARKS

A study of a bang-bang controller for longitudinal- and lateral-range control of an entry from supercircular velocities has been made. A random number procedure was used to determine the effect upon the range control of assumed measurement error in velocity, altitude, and rate of change of altitude.

The results of this study show that the controller was capable of controlling angular ranges, from the point of entry to a terminal altitude of 30,000 meters, between 18° and 250°.

The range controller is about an order of magnitude more sensitive to measurement errors when a medium- or long-range entry is desired than when a short-range entry is desired.

Langley Research Center,
National Aeronautics and Space Administration,
Langley Station, Hampton, Va., June 8, 1967,
125-17-05-01-23.

REFERENCES

1. Wingrove, Rodney C.: A Survey of Atmosphere Re-Entry Guidance and Control Methods. AIAA J., vol. 1, no. 9, Sept. 1963, pp. 2019-2029.

2. White, Jack A.: Feasibility Study of a Bang-Bang Path Control for a Reentry Vehicle. NASA TN D-2049, 1963.
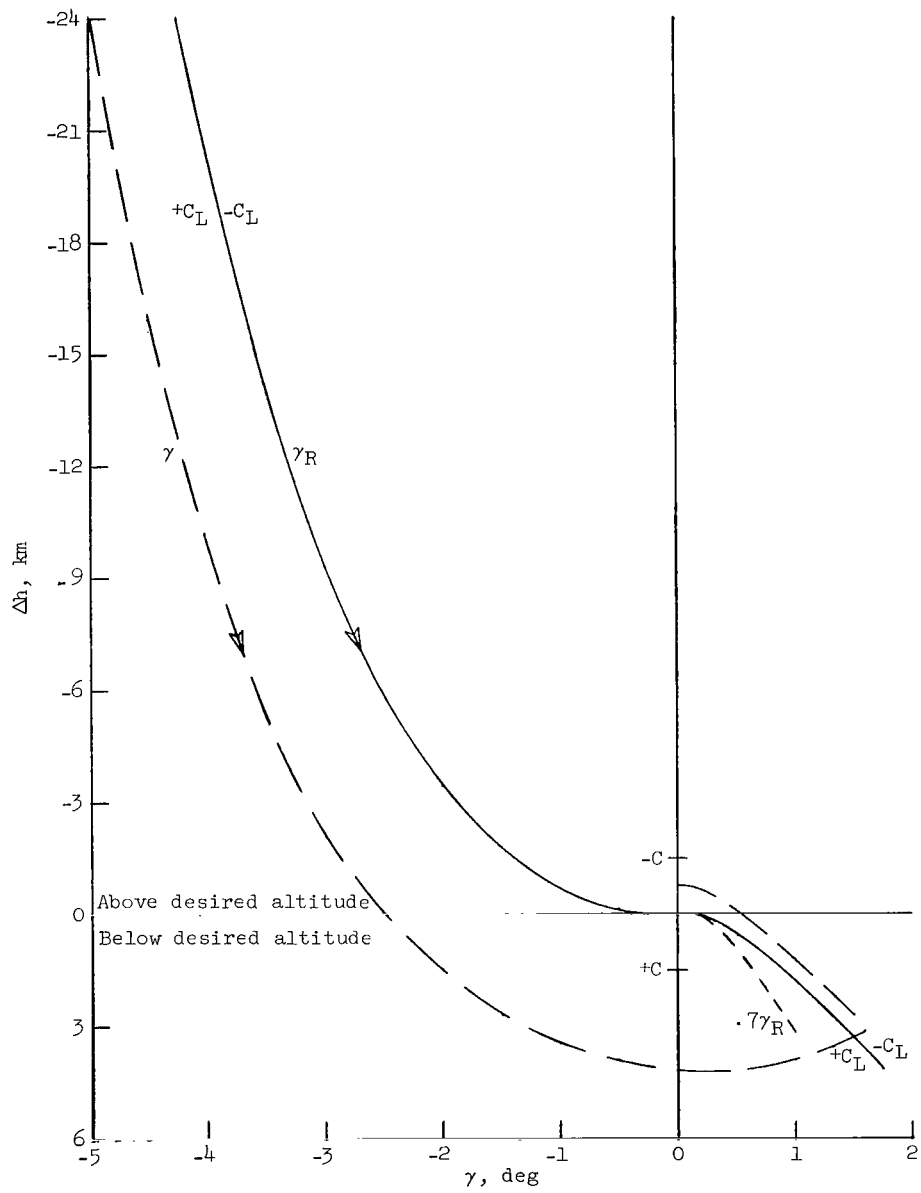
Figure 1.- Bang-bang switching curve for a typical entry.
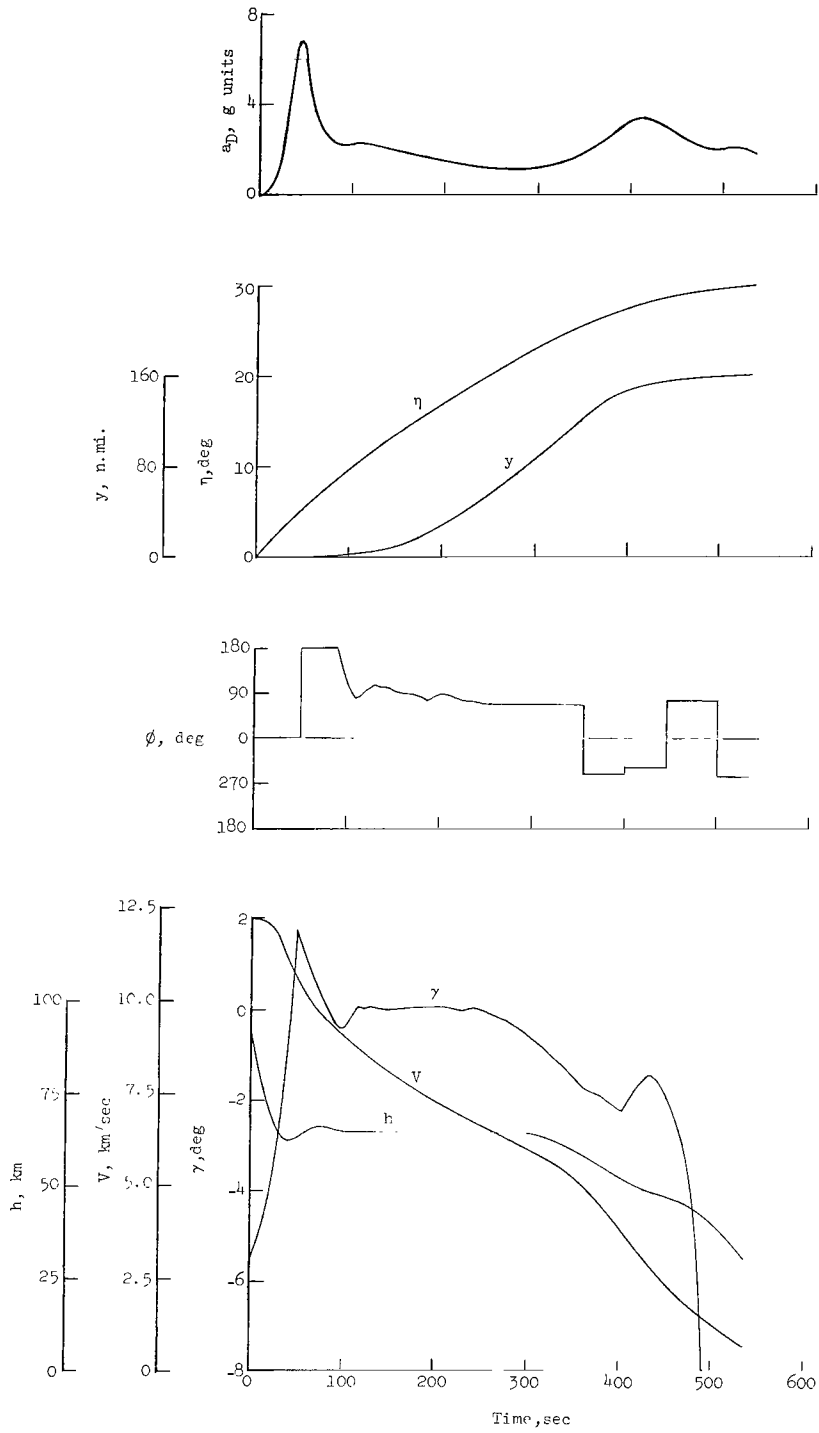
Figure 2.- Typical time history of a direct descent entry trajectory (Mode I). γ_0 = -5.5°; V_0 = 12.2 km/sec; h_0 = 91.44 km; η_d = 30°; y_d = 160 n. mi.
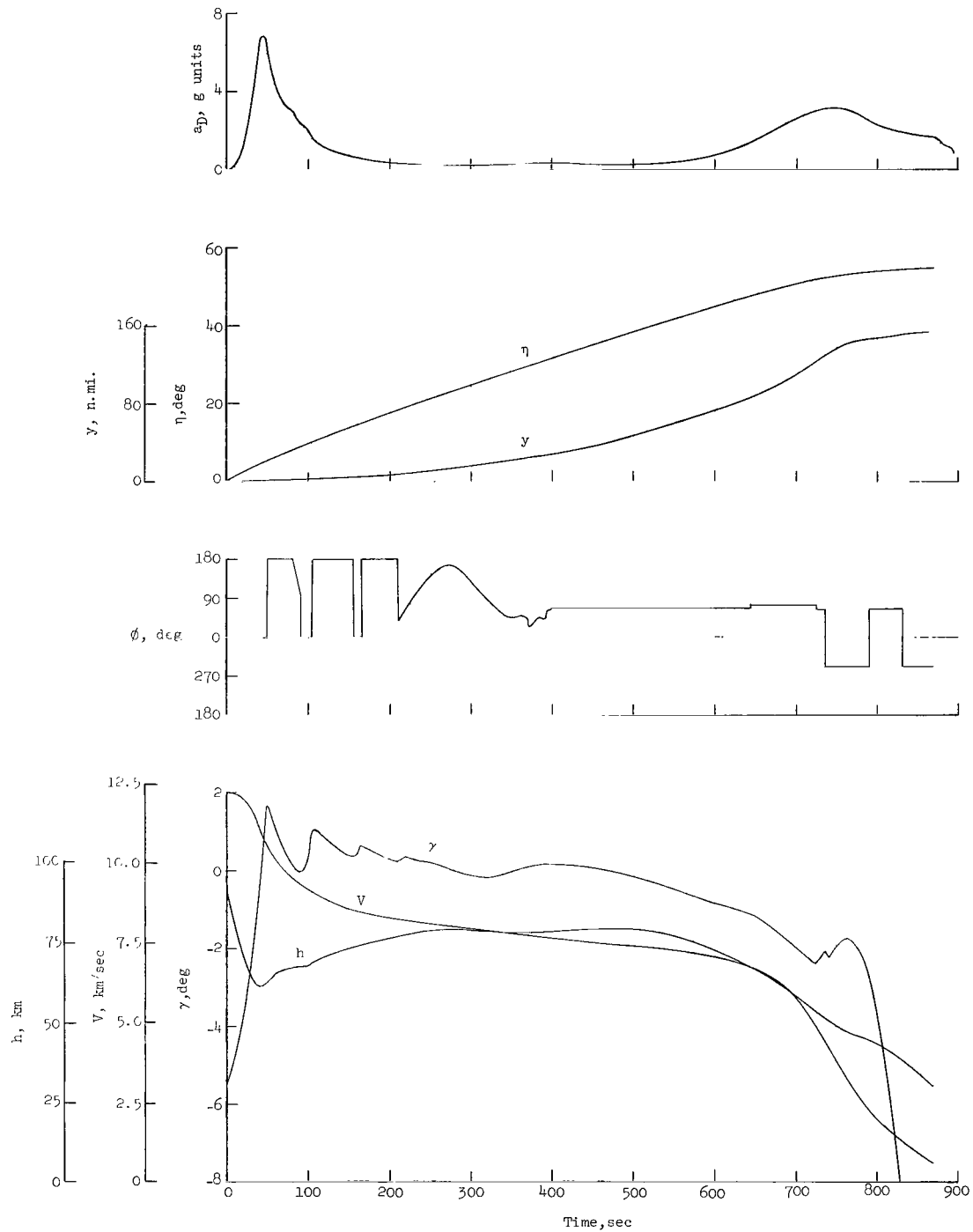
Figure 3.- Typical time history of a medium-range entry trajectory (Mode II). $\gamma = -5.5^\circ$; $V_0 = 12.2$ km/sec; $h_0 = 91.44$ km; $\eta_d = 55^\circ$; $y_d = 160$ n. mi.

19
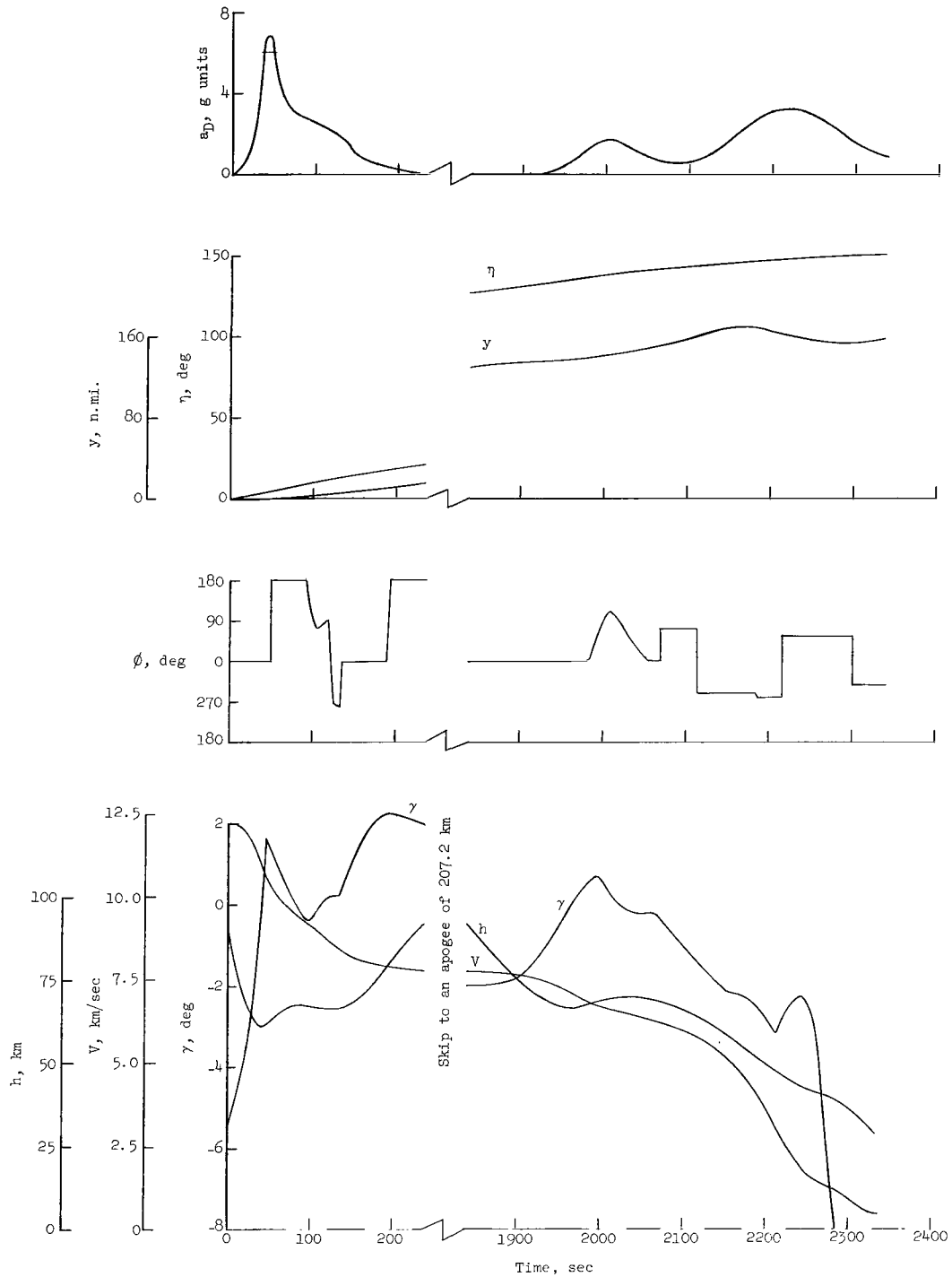
Figure 4.- Typical time history of a long-range entry trajectory (Mode III). $\gamma = -5.5^0$; $V_0 = 12.2$ km/sec; $h_0 = 91.44$ km; $\eta_d = 150^0$; $y_d = 160$ n. mi.
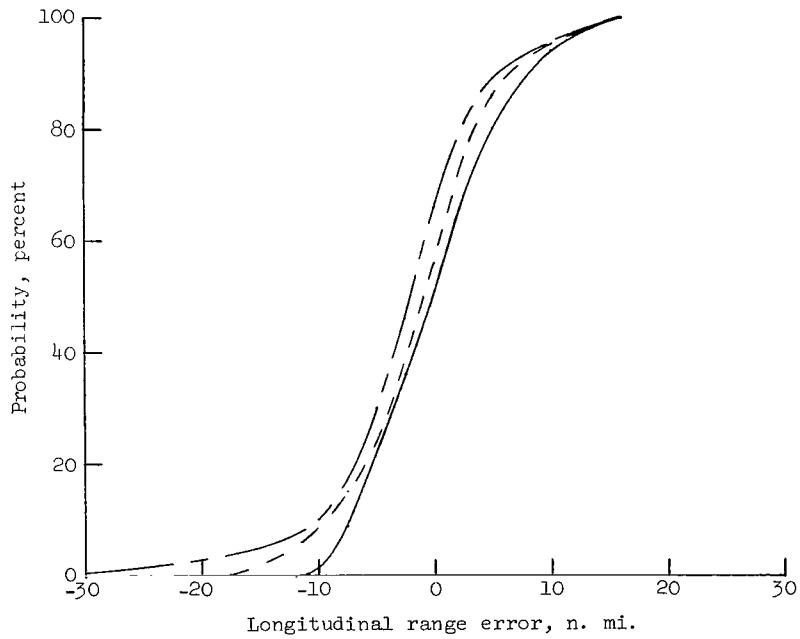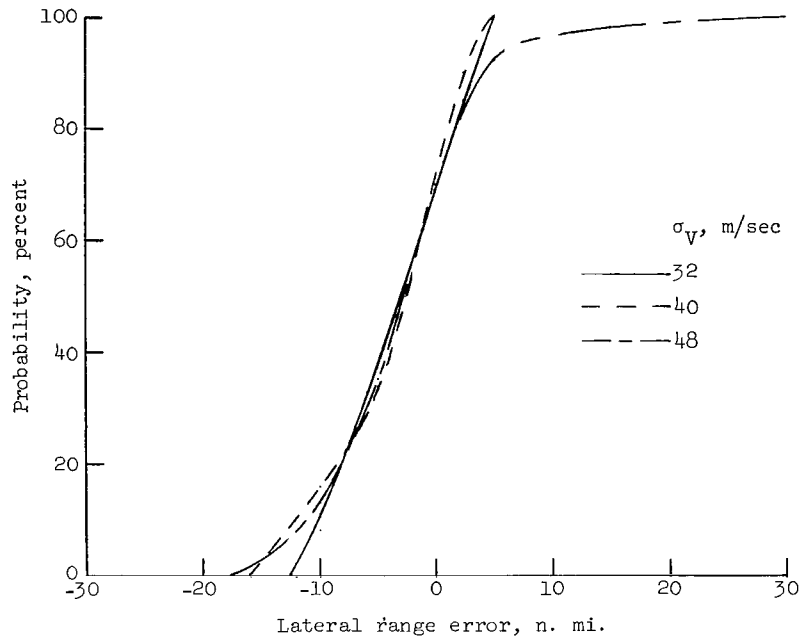
(a) Effect of varying σ_V while $\sigma_h = 0$ and $\sigma_{\dot{h}} = 0$.

Figure 5.- Probability-distribution curves of longitudinal and lateral range errors for direct descent entries. $\eta_d = 30°$; $y_d = 160$ n. mi.
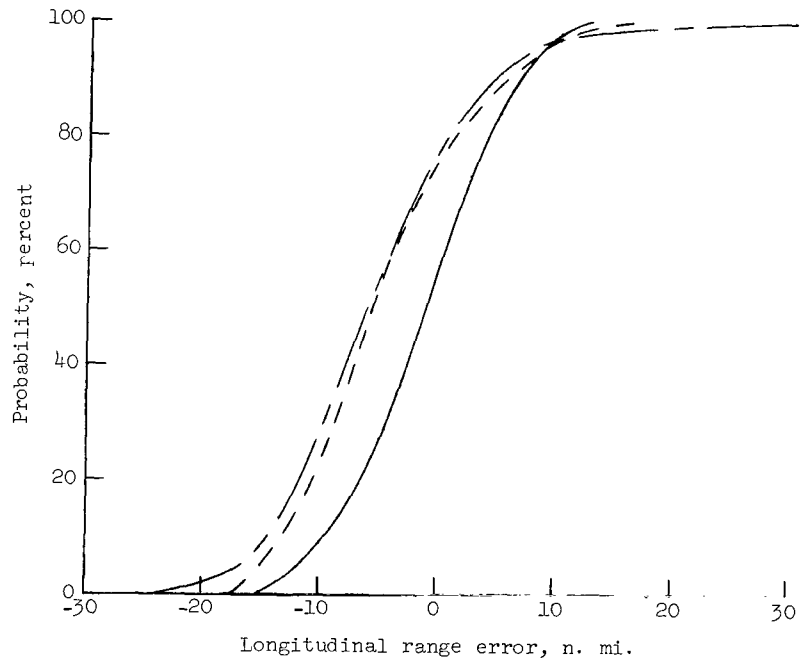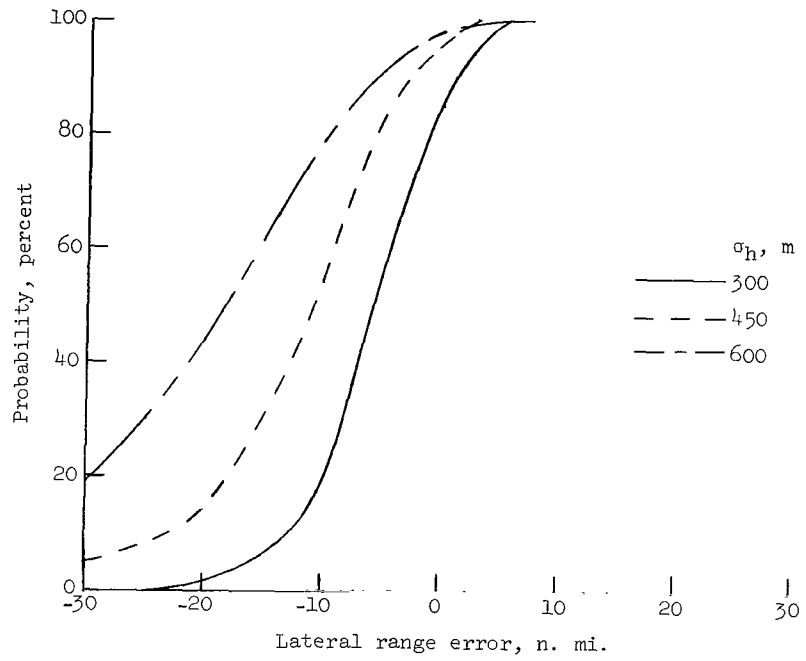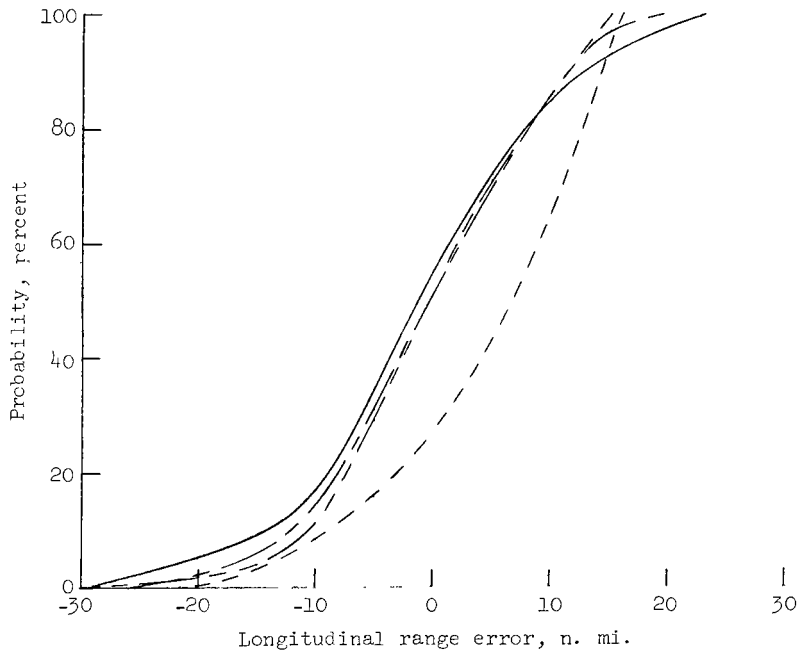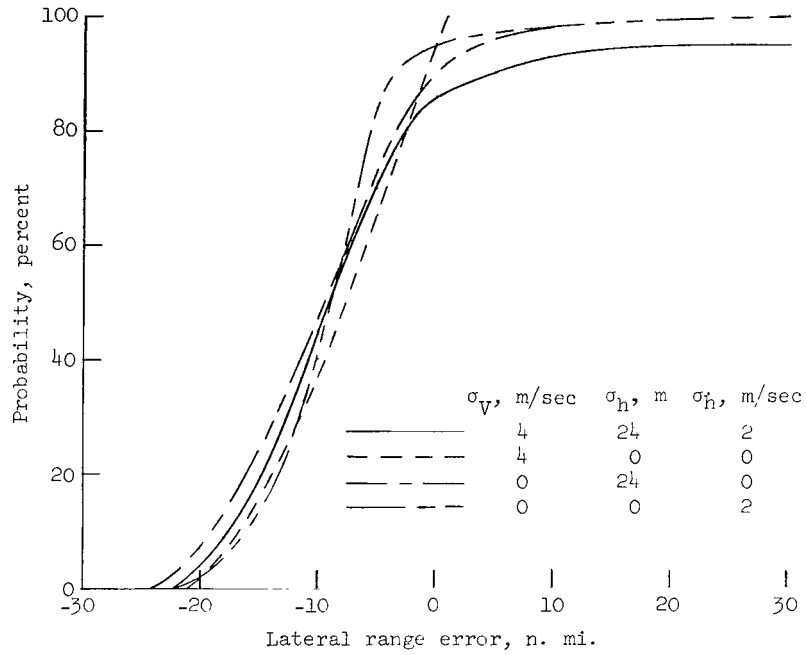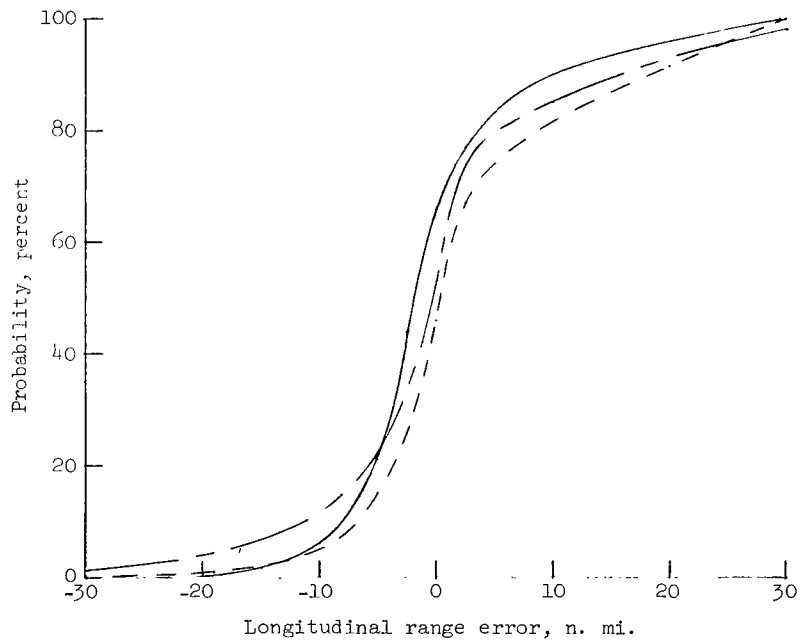
(b) Effect of varying σ_h while $\sigma_V = 0$ and $\sigma_h' = 0$.
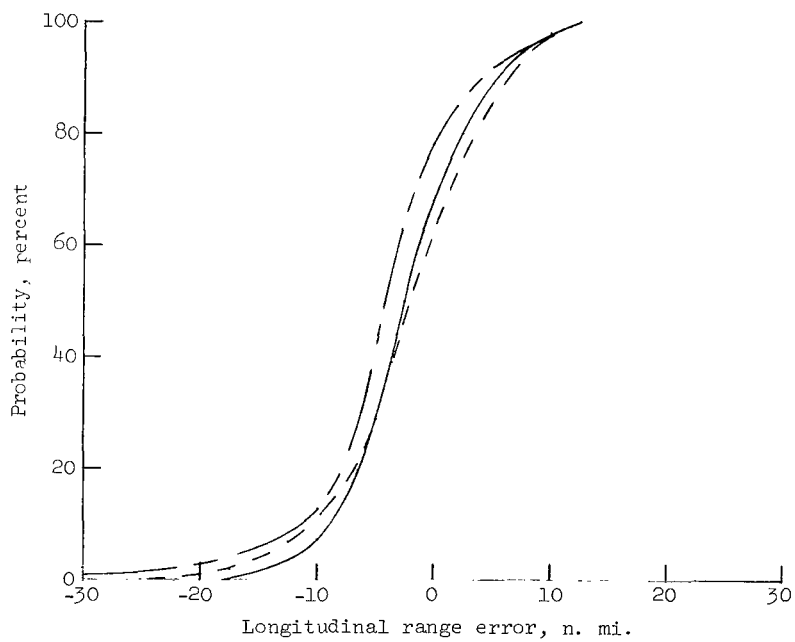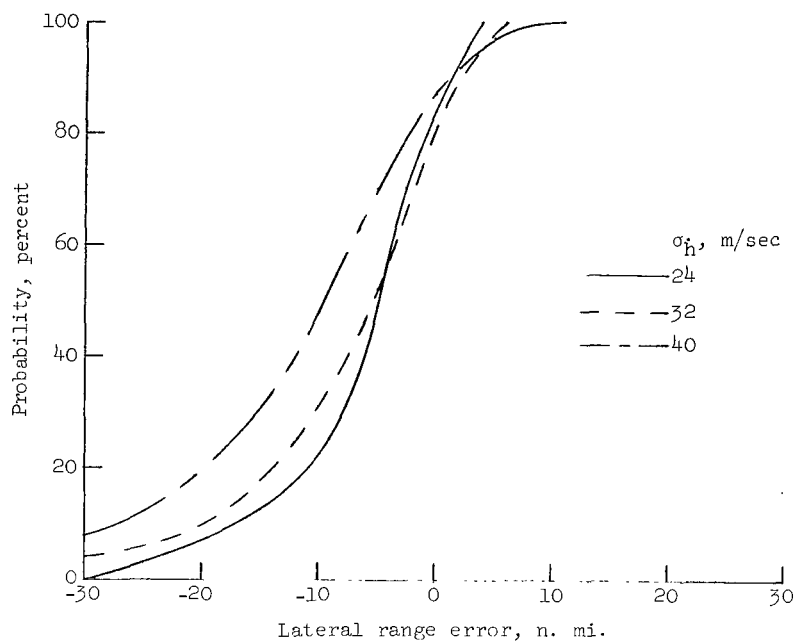
Figure 5.- Continued.

(c) Effect of varying $\sigma_{\dot{h}}$ while $\sigma_V = 0$ and $\sigma_{\dot{h}} = 0$.

Figure 5.- Continued.
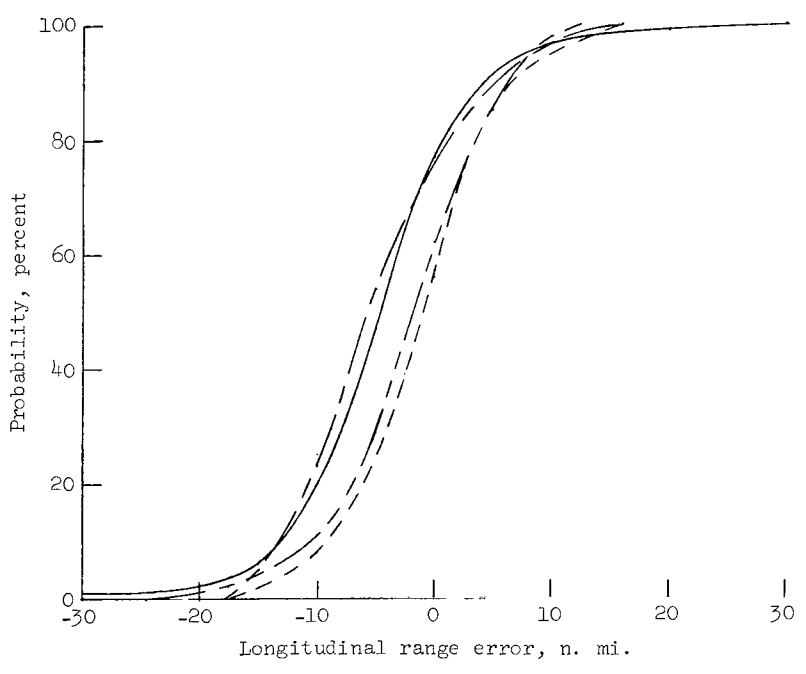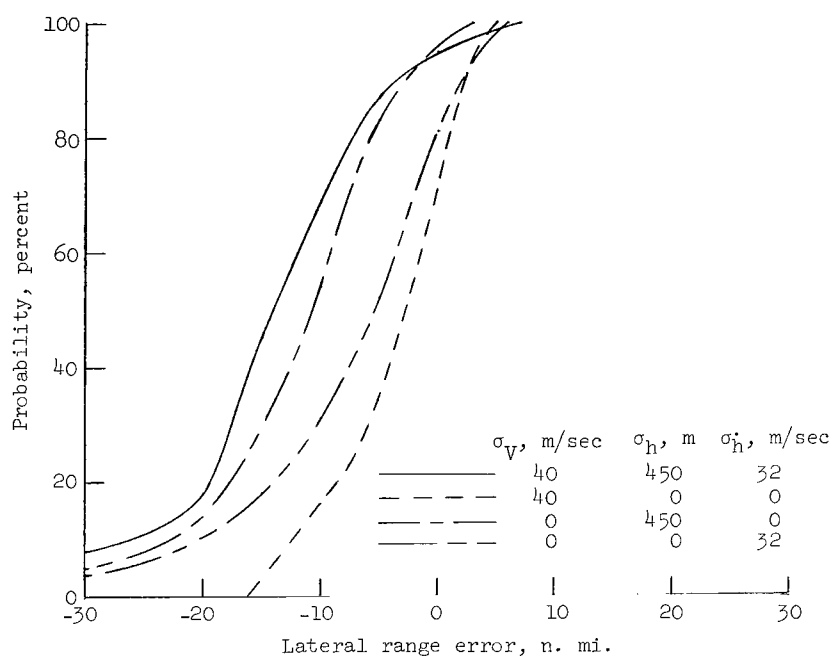
(d) Combined effect of errors in σ_V, σ_h, and $\sigma_{\dot{h}}$.

Figure 5.- Concluded.
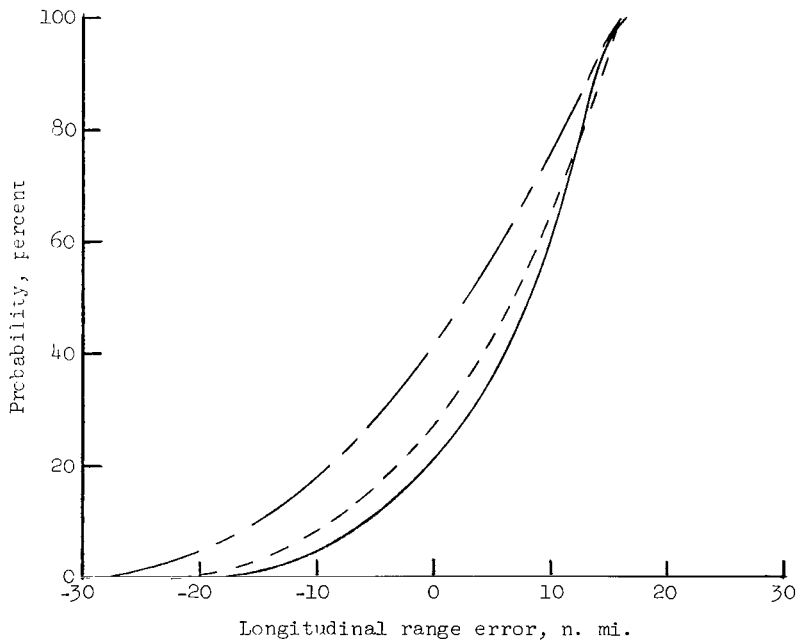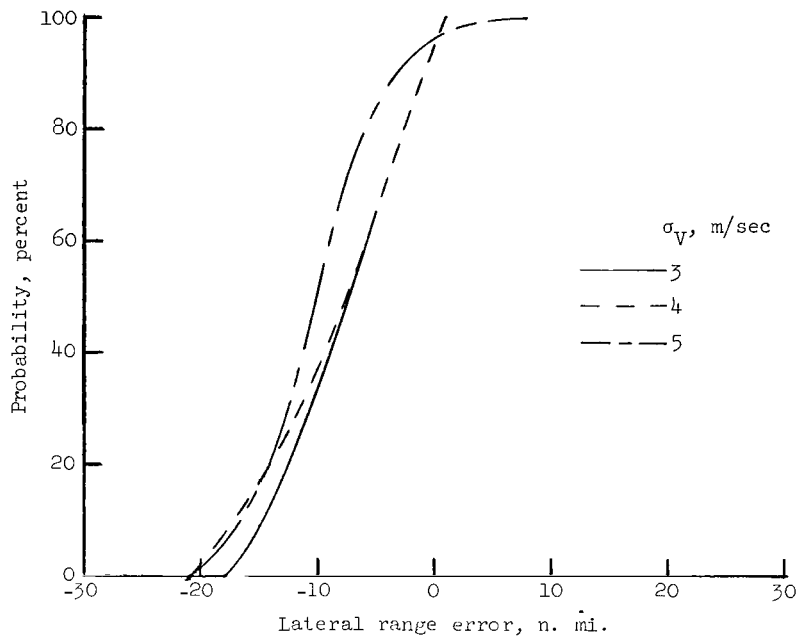
(a) Effect of varying σ_V while $\sigma_h = 0$ and $\sigma_{\dot{h}} = 0$.

Figure 6.- Probability-distribution curves of longitudinal and lateral range errors for medium-range entries. $\eta_d = 55^0$; $y_d = 160$ n. mi.

(b) Effect of varying σ_h while $\sigma_V = 0$ and $\sigma_{\dot h} = 0$.
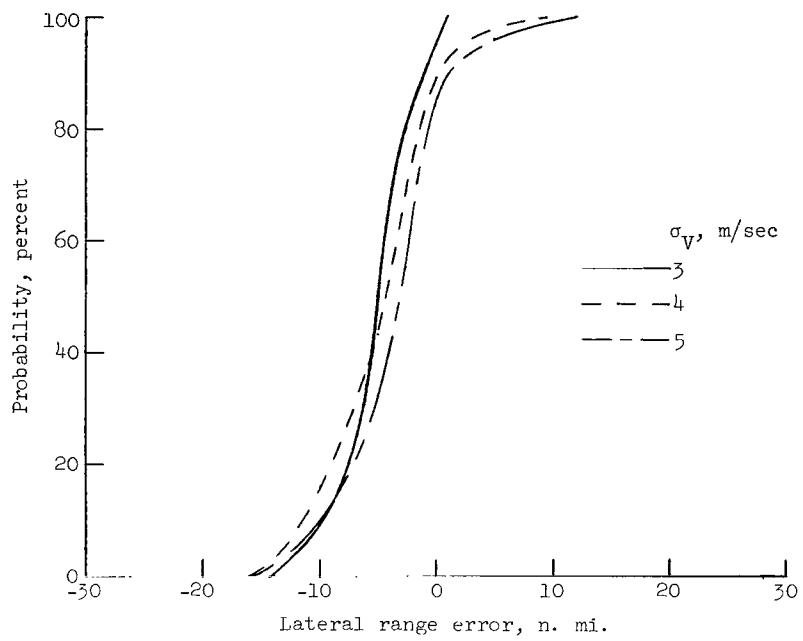
Figure 6.- Continued.

26

(c) Effect of varying σ_h while $\sigma_v = 0$ and $\sigma_h = 0$.
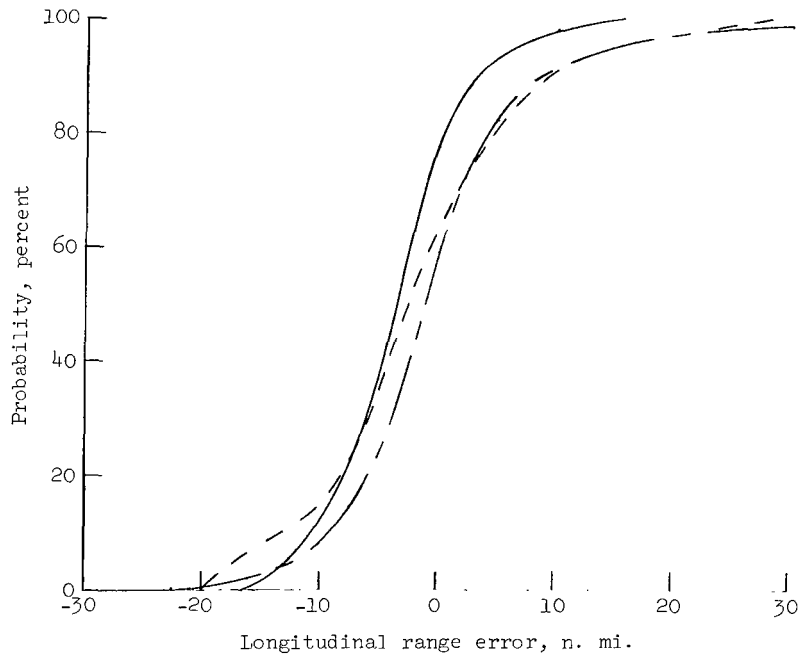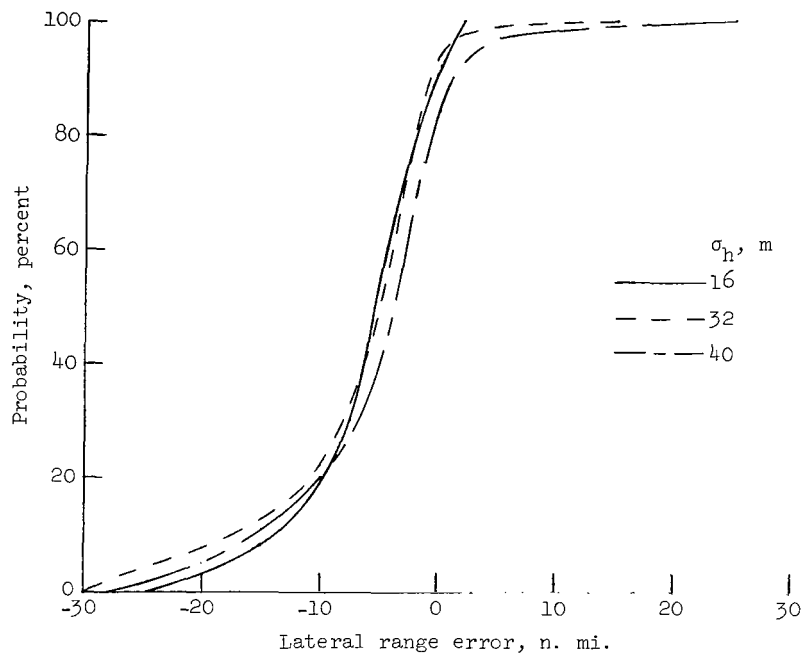
Figure 6.- Continued.

Probability, percent

σ_V, m/sec σ_h, m $\sigma_{\dot h}$, m/sec
4   24   2
4   0   0
0   24   0
0   0   2

-30   -20   -10   0   10   20   30

Lateral range error, n. mi.

Probability, percent

-30   -20   -10   0   10   20   30

Longitudinal range error, n. mi.

(d) Combined effect of errors in σ_V, σ_h, and $\sigma_{\dot h}$.
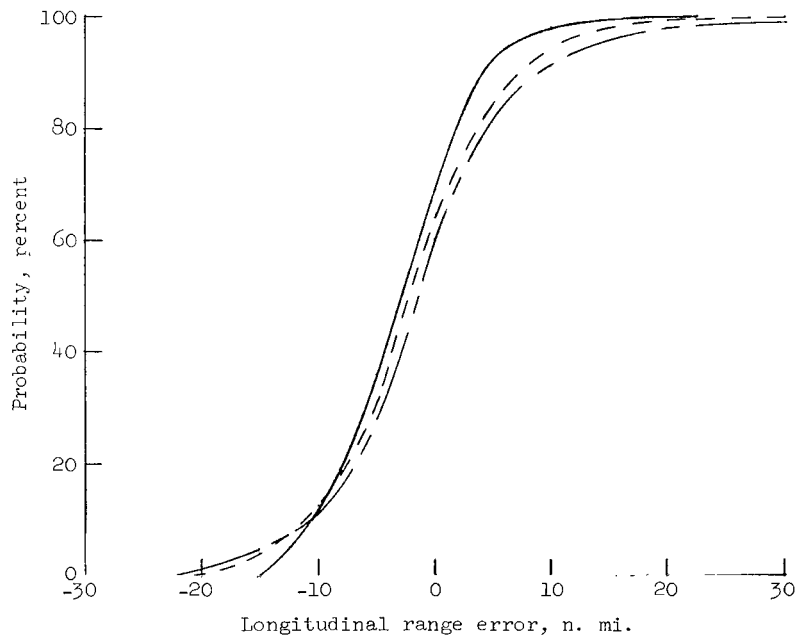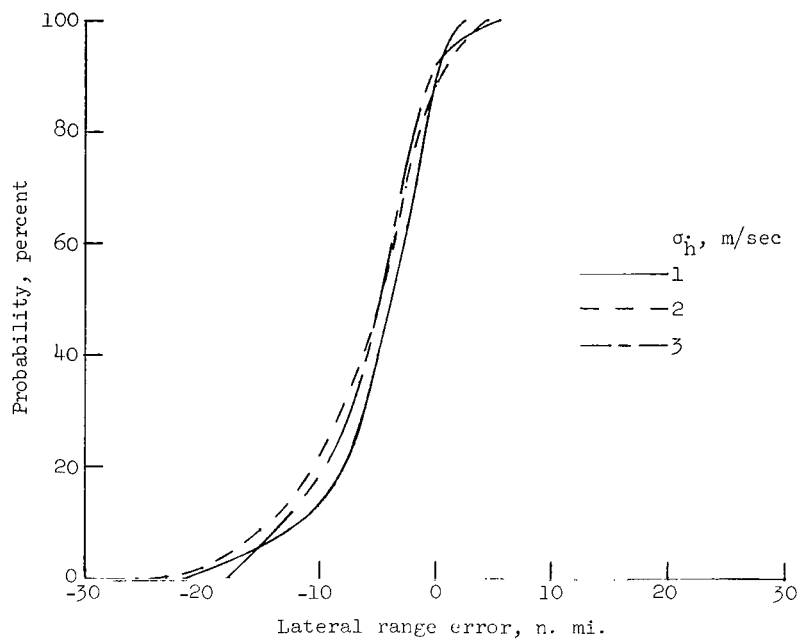
Figure 6.- Concluded.

(a) Effect of varying σ_V while $\sigma_h = 0$ and $\sigma_h' = 0$.

Figure 7.- Probability-distribution curves of longitudinal and lateral range errors for long-range entries. $\eta_d = 150^0$; $y_d = 160$ n. mi.
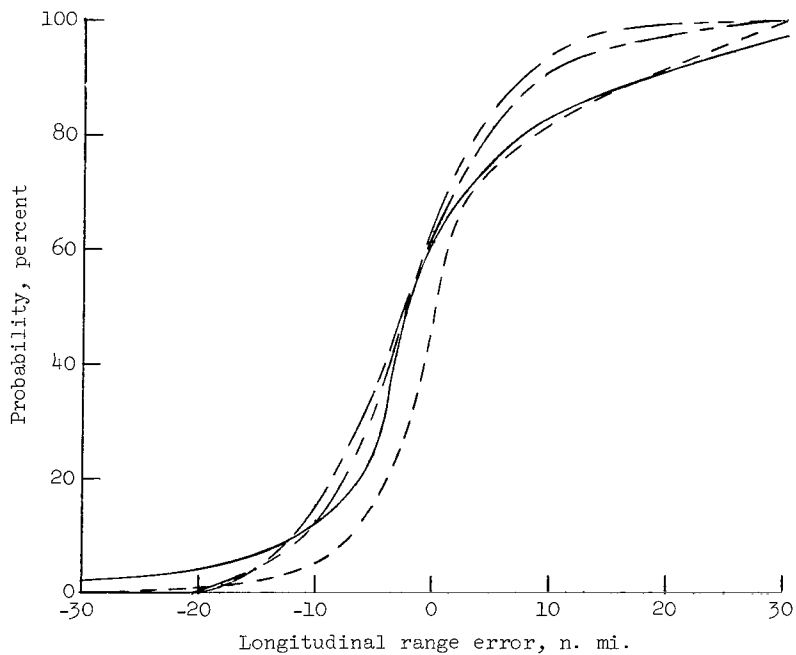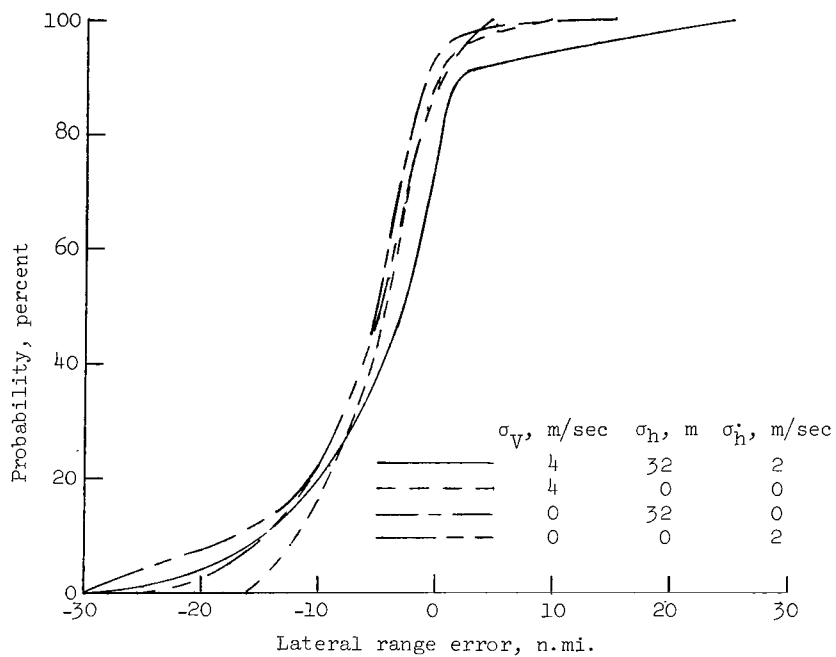
(b) Effect of varying σ_h while $\sigma_v = 0$ and $\sigma_{\dot{h}} = 0$.

Figure 7.- Continued.

(c) Effect of varying $\sigma_{\dot{h}}$ while $\sigma_v = 0$ and $\sigma_{\dot{h}} = 0$.

Figure 7.- Continued.

	σ_V, m/sec	σ_h, m	$\sigma_{\dot{h}}$, m/sec
	4	32	2
	4	0	0
	0	32	0
	0	0	2

Lateral range error, n.mi.

Longitudinal range error, n. mi.

(d) Combined effect of errors in σ_V, σ_h, and $\sigma_{\dot{h}}$.

Figure 7.- Concluded.

NASA SCIENTIFIC AND TECHNICAL PUBLICATIONS

TECHNICAL REPORTS: Scientific and technical information considered important, complete, and a lasting contribution to existing knowledge.

TECHNICAL NOTES: Information less broad in scope but nevertheless of importance as a contribution to existing knowledge.

TECHNICAL MEMORANDUMS: Information receiving limited distribution because of preliminary data, security classification, or other reasons.

CONTRACTOR REPORTS: Scientific and technical information generated under a NASA contract or grant and considered an important contribution to existing knowledge.

TECHNICAL TRANSLATIONS: Information published in a foreign language considered to merit NASA distribution in English.

SPECIAL PUBLICATIONS: Information derived from or of value to NASA activities. Publications include conference proceedings, monographs, data compilations, handbooks, sourcebooks, and special bibliographies.

TECHNOLOGY UTILIZATION PUBLICATIONS: Information on technology used by NASA that may be of particular interest in commercial and other non-aerospace applications. Publications include Tech Briefs, Technology Utilization Reports and Notes, and Technology Surveys.

Details on the availability of these publications may be obtained from:

SCIENTIFIC AND TECHNICAL INFORMATION DIVISION

NATIONAL AERONAUTICS AND SPACE ADMINISTRATION

Washington, D.C. 20546